CHEMISTRY

A EUROPEAN JOURNAL

ChemPubSoc Europe

Reprint

Supported by ACES

WILEY-VCH

www.chemeurj.org

CHEMISTRY
A EUROPEAN JOURNAL

GERMANY NETHERLANDS
BELGIUM ITALY
FRANCE SPAIN
PORTUGAL GREECE
CZECH REP. POLAND

REPRINT

DNA

2012 – 18/43

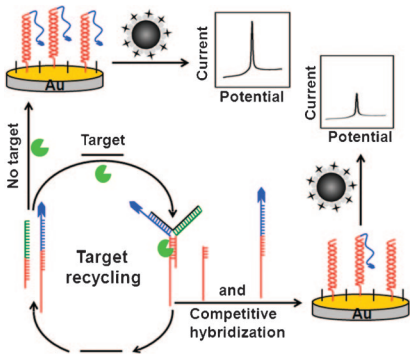

Sense-ational: A competitive strategy was designed for ultrasensitive detection of sequence-specific DNA by combining homogeneous endonuclease-assisted target DNA recycling with streptavidin-functionalized silver-nanoparticle-tagged carbon nanospheres as electrochemical labels (see figure). The sensing strategy showed excellent performance.

SWEDEN HUNGARY
AUSTRIA

WILEY-VCH

CHEMISTRY
A EUROPEAN JOURNAL

FULL PAPER

DOI: 10.1002/chem.201201307

A Competitive Strategy Coupled with Endonuclease-Assisted Target Recycling for DNA Detection Using Silver-Nanoparticle-Tagged Carbon Nanospheres as Labels

Zhu Zhu, Fenglei Gao, Jianping Lei, Haifeng Dong, and Huangxian Ju*[a]

Abstract: A simple competitive strategy was designed for the sensitive detection of sequence-specific DNA by combining endonuclease-assisted target recycling and electrochemical stripping analysis of silver nanoparticles (AgNPs). The AgNP-tagged carbon nanospheres were synthesized by means of in situ reduction of Ag^+ adsorbed onto a negatively charged polyelectrolyte layer and functionalized with streptavidin for binding biotin-labeled DNA strands. The labeled strand was captured on the DNA sensor surface by competitive hybridization of biotinated primer 1 and its cleaved product. The cleaved product could be amplified in homogeneous solution by endonuclease-assisted target recycling with a Y-shaped junction DNA structure, thus leading to the correlation of the stripping signal to the target concentration. The functionalized nanosphere was characterized with X-ray photoelectron spectroscopy, scanning electron microscopy, and transmission electron microscopy. The proposed method showed a linear range from 0.1 to 1000 fM with a limit of detection of 0.066 fM (3σ) and good selectivity for base discrimination. The designed strategy provided a sensitive tool for DNA analysis and could be widely applied in bioanalysis and biomedicine.

Keywords: DNA · enzymes · sensors · silver · nanoparticles

Introduction

Sensitive and selective approaches for DNA detection have been rapidly developed over the past decades due to the needs in a variety of areas including clinical diagnostics, food safety, and environmental protection.[1–7] Many efforts have been devoted to the design of signal amplification strategies for realizing ultrasensitive and even close to single-molecule detection. Generally, signal amplification can be performed by loading a large number of signal molecules on a nanocarrier for labeling the recognition molecule.[8–10] Recently, target DNA recycling as an isothermal signal amplification strategy[11–13] that uses various nucleases—for example, endonuclease,[3,14–18] polymerase,[19–21] and exonuclease[22–24]—has attracted considerable attention. The proposed methods can produce strong detectable signals for the analysis of trace levels of target DNA with specific sequences.

The signal molecules loaded on nanocarriers include enzymes or nanoparticles (NPs). The abundant enzyme molecules assembled on a sensor surface can efficiently catalyze related reactions to produce excited species for optical detection or electroactive molecules for electrochemical analysis.[25] The NPs assembled on nanocarriers can be detected by using different analytical techniques coupled with various pretreatments after being captured by the immobilized recognition molecules. For example, CdTe NPs loaded on poly(styrene-*co*-acrylic acid) microbeads can be dissolved with acid and then detected with electrochemical stripping analysis.[26] These nanocarrier-based signal amplification strategies greatly improve the detection sensitivity of DNA targets or proteins. Thus various materials such as dendrimers,[10] silica NPs,[25] carbon nanotubes,[27] and gold NPs[28] have been used as the nanocarriers to load the signal molecules. Recently, carbon nanospheres (CNSs) have also become excellent candidates for these nanocarriers[29–31] by virtue of their high chemical stability, and their convenient and absolutely "green" preparation.[32] Since the as-formed CNSs inherit a large number of functional groups from the starting materials and have reactive surfaces, AuNPs[29,31] and enzymes[30] can be assembled on their surface as an electrochemical tag for the detection of biomolecules. This work used CNSs as a nanocarrier to assemble AgNPs using a layer-by-layer technique and in situ reduction of Ag^+. The AgNP-tagged CNS was then functionalized with streptavidin and used as a signal mark for ultrasensitive detection of DNA with the aid of the endonuclease-assisted target recycling and competitive hybridization of biotin-labeled DNA strand to a DNA sensor.

Endonuclease-assisted genosensing can be conveniently performed for signal amplification by target recycling, especially in the homogeneous format of an enzymatic reaction. However, since the targets should contain cleavage sites with specific sequences for endonuclease recognition, the application of these approaches is limited. To avoid the

[a] Z. Zhu, F. Gao, Dr. J. Lei, Dr. H. Dong, Prof. H. Ju
State Key Laboratory of Analytical Chemistry
for Life Science
School of Chemistry and Chemical Engineering
Nanjing University, Nanjing 210093 (P.R. China)
Fax: (+86) 25-8359-3593
E-mail: hxju@nju.edu.cn

need for specific target sequences for endonuclease recognition, Sintim and co-workers[33] proposed a so-called "template-enhanced hybridization process" for isothermal amplified detection of nucleic acids by forming a Y-shaped junction DNA that consists of three complementary oligonucleotide branches, in which the cleavage site is located on the branch independent of target sequences. Therefore, this method can overcome the disadvantage of endonuclease recognition. It has been used for DNA detection on a gold electrode by using methylene blue as a signal molecule.[34] Here, in the presence of an endonuclease, the Y-shaped junction DNA structure could produce a target-sequence-independent product and release the target DNA. The released target further hybridized with primers 1 and 2 to trigger another cycle of cleavage and produce more target-sequence-independent DNA strands (Scheme 1). With a de-

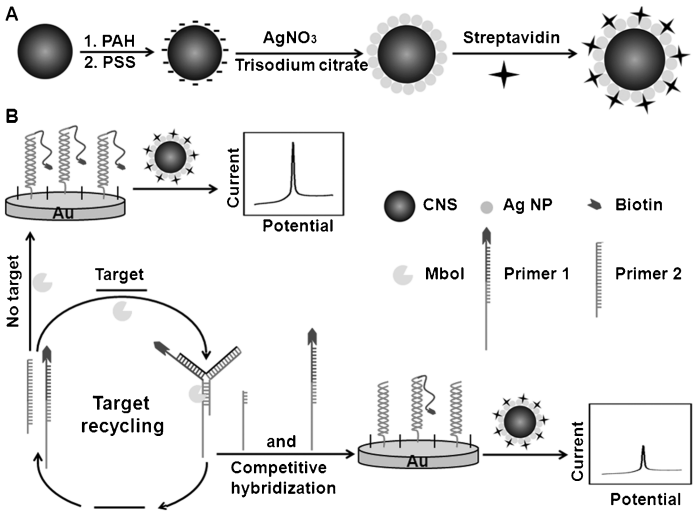

Scheme 1. A) Schematic diagram of the preparation of streptavidin/AgNP-tagged CNSs. B) Illustration of the detection strategy by means of endonuclease-assisted target DNA recycling and streptavidin-functionalized AgNP-tagged CNSs as label.

signed competitive hybridization of the DNA strand cleaved by endonuclease-assisted target recycling amplification and biotin-labeled primers 1 to capture probes immobilized on sensor surfaces, a simple electrochemical detection method for DNA was proposed by combination with streptavidin-functionalized AgNP-tagged CNSs as a label. By integrating the homogeneous enzymatic reaction with the electrochemical stripping of AgNPs, this method showed a sub-femtomolar detection limit of the target DNA with a wide linear range and good selectivity for base discrimination. The designed competitive strategy could be applied to ultrasensitive bioanalysis of DNA.

Results and Discussion

Principle of the sensing system: As shown in Scheme 1, primer 1 labeled with biotin at the 5′ end contained three regions from 5′ to 3′, which are complementary to parts of the target, primer 2, and capture probe. The part of primer 1 that hybridizes with primer 2 contains a 4-mer sequence (5′GATC3′) that is the site of the MboI restriction endonuclease. Unlabeled primer 2 contains two regions that are complementary to the remaining segment of target DNA and the 5′TTTGATC3′ sequence in primer 1. MboI only cleaves double-stranded DNA, therefore primer 1 cannot be cleaved by MboI unless the segment hybridizes with primer 2 to form a duplex. In fact, the short complementary duplex formed by the hybridization of primer 1 and primer 2 in the absence of target DNA is thermodynamically unstable;[33] MboI does not cleave the single strands of both primers 1 and 2. In the presence of a target as a DNA-assisted template, primers 1 and 2 and the target can hybridize to form a ternary Y-junction structure. This structure contains the MboI site, which leads to the cleavage of primer 1 to produce target-sequence-independent DNA strands. The cleavage also results in the low stability of the remaining structure, and thus releases the target. The released target can then further hybridize with primers 1 and 2 to trigger another cycle of cleavage. Hence the recycling of the target can produce a large number of target-sequence-independent DNA strands, which can hybridize with the capture probe immobilized on the sensor surface competitively with the biotin-labeled primers 1. The amount of the biotin group captured on the sensor surface correlated negatively with the concentration of target.

After the streptavidin-functionalized AgNP-tagged CNS was immobilized on the sensor surface by means of the interaction between captured biotin and streptavidin, the amount of AgNPs can be detected by performing a linear potential sweep from −0.15 to 0.20 V at 50 mV s^{-1} in 1.0 M KCl solution. The stripping peak current is also correlated negatively with the concentration of target DNA.

Characterization of functional AgNP-tagged CNSs: The CNSs were obtained by a hydrothermal synthetic approach.[32] The negatively charged groups on the CNS surface were then used for layer-by-layer assembly of poly(allylamine hydrochloride), poly(sodium 4-styrenesulfonate), and Ag^+. Subsequently, the AgNP-tagged CNSs were prepared by in situ chemical deposition of AgNPs in the presence of trisodium citrate as illustrated in Scheme 1A. Figure 1 shows the scanning electron microscopy (SEM) and transmission electron microscopy (TEM) images of the CNSs and AgNP-tagged CNSs. The CNSs showed a homogeneous and smooth surface and good dispersion with a narrow size distribution. The average diameter of the CNSs was about 100 nm (Figure 1A). Relative to bare CNS, the SEM image of the AgNP-tagged CNS showed an island structure on the surface due to the deposition of AgNPs (Figure 1B). High-resolution TEM images clearly indicated that dense AgNPs were loaded on the surface of CNSs (Figure 1C and D).

X-ray photoelectron spectroscopy (XPS) and Fourier transform infrared (FTIR) spectra were also used to charac-

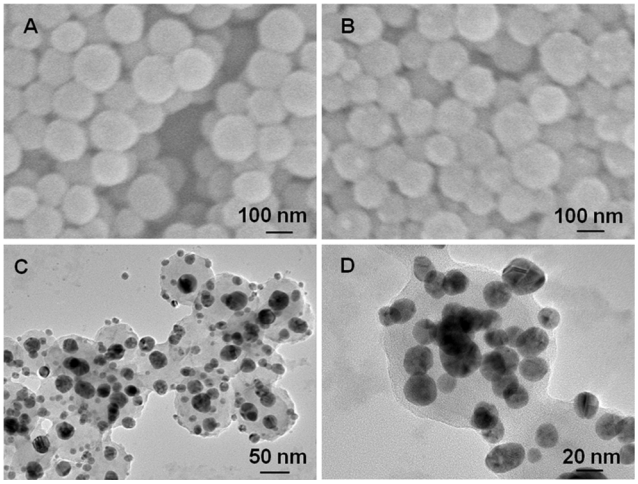

Figure 1. SEM images of A) CNSs, B) AgNP-tagged CNSs, and C,D) TEM images of AgNP-tagged CNSs.

terize the AgNP-tagged CNSs (Figure 2). The XPS spectra showed several strong peaks at 284, 368, 374, 532, 573, and 604 eV, which correspond to C 1s, Ag $3d_{5/2}$, Ag $3d_{3/2}$, O 1s, Ag $3p_{3/2}$, and Ag $3p_{1/2}$, respectively (Figure 2A). This result

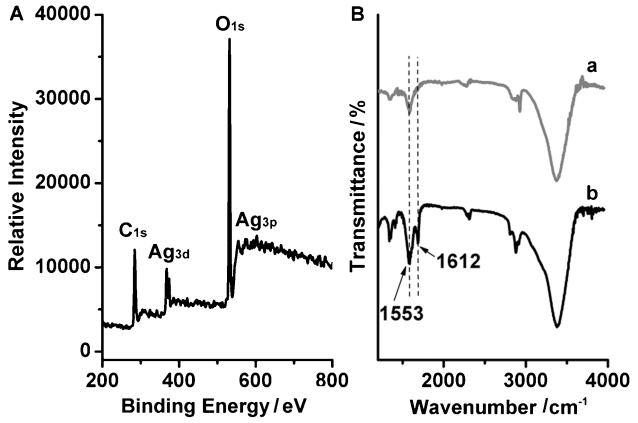

Figure 2. A) XPS spectrum of AgNP-tagged CNSs. B) FTIR spectra of bare (curve a) and streptavidin-functionalized AgNP-tagged CNSs (curve b).

further confirmed that the AgNPs were successfully loaded onto the surface of CNS. In comparison with AgNP-tagged CNSs (Figure 2B, curve a), the FTIR spectrum of streptavidin-functionalized AgNP-tagged CNSs displayed clear absorption peaks that corresponded to the amide bands I (1612 cm^{-1}) and amide bands II (1553 cm^{-1}) of streptavidin (Figure 2B, curve b), which indicated that the streptavidin was successfully linked to the surface of AgNP-tagged CNSs.

Optimization and electrochemical characterization of the DNA sensor: Generally, the density of the DNA probe immobilized on the sensor surface is one of the most important parameters to impact the sensing response.[35] That is, a low density leads to a low response, whereas a high density might also decrease the response due to the steric blocking of DNA hybridization and the binding of tags. The density of the probe self-assembled on a gold electrode increases along with the assembly time and its concentration. As shown in Figure 3A, at the self-assembly time of 3 h, the response increased along with the increasing concentration of the capture probe and reached the maximum value at 2.0 μM. Therefore, 2.0 μM was used as the optimized concentration of the capture probe.

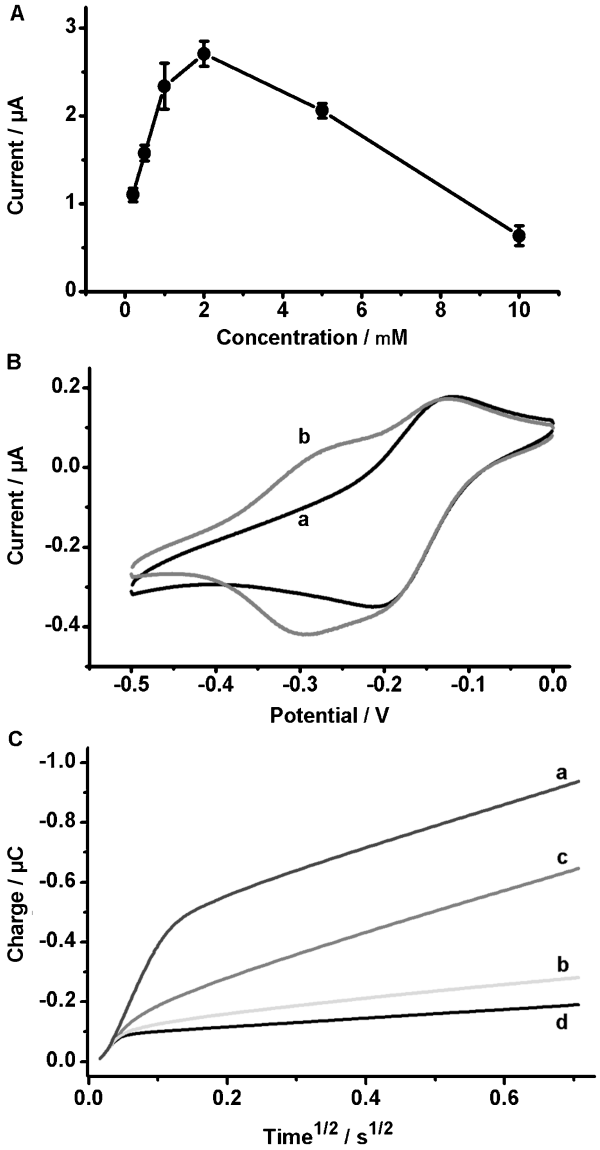

Figure 3. A) Dependence of the stripping peak current of captured streptavidin-functionalized AgNP-tagged CNSs on the concentration of the capture probe used for sensor preparation. Target: 1 pM, MboI digesting: 1 h at 37 °C. B) Cyclic voltammograms of 50 μM RuHex at a) MCH and b) capture probe-/MCH-modified electrodes at 50 mV s^{-1} in 10 mM Tris-HCl (pH 7.0). C) Chronocoulometric responses of a,b) capture probe-/MCH- and c,d) MCH-modified electrodes with a potential step from 100 to −400 mV in the b,d) absence and a,c) presence of 50 μM RuHex in 10 mM Tris-HCl (pH 7.0).

The DNA monolayer was further characterized with cyclic voltammetry and chronocoulometry by electrostatically binding hexaammineruthenium(III) chloride (RuHex) to the immobilized single-strand DNA at low ionic strength. The surface density of the DNA probe could be calculated by comparing the redox charges of RuHex at the 6-mercaptohexanol (MCH)-assembled gold electrode and DNA-probe-modified gold electrode blocked with MCH.[36,37] A pair of well-defined peaks that corresponded to the reduction and oxidation of RuHex were observed at the MCH-coated electrode surface (Figure 3B, curve a), whereas the probe-modified electrode showed two pairs of peaks (Figure 3B, curve b). The second pair of peaks at about −0.3 V was characteristic of a surface-confined redox process due to the closed peak separation, which was due to the binding of cationic RuHex to the anionic phosphate backbone of DNA, thus demonstrating the assembly of the capture probe on the surface as anticipated. By comparison of the chronocoulometric curves at the MCH-modified electrode (Figure 3C, curves c and d), it could be concluded that the nonspecific adsorption of RuHex at the electrode surface was negligible, because the intercepts were nearly identical in the presence and absence of the redox probe. The surface excess amount of RuHex at the capture probe-/MCH-modified electrode was thus calculated from the difference of response intercepts in the absence and presence of the redox probe (Figure 3C, curves a and b), which suggested the surface density of the DNA probe to be about 5×10^{12} mol cm^{-2}.[37]

Optimal conditions for endonuclease-assisted target recycling: The reaction conditions, including reaction temperature and time, influenced the performance of the proposed strategy. The reaction temperature was pivotal to the formation of a Y-junction structure and the cleavage of primer 1 in the presence of MboI. At relatively low temperature, primers 1 and 2 would hybridize even in the absence of target, which resulted in the subsequent cleavage, thus producing a low stripping peak current (Figure 4A). In the presence of target DNA, the stripping peak showed only a slight decrease, thus indicating low target recycling efficiency. On the contrary, at relatively high temperature, the Y-junction structure was not stable enough to produce the MboI-catalyzed cleavage. Thus the stripping current at the target concentration of 1 pM was almost as high as that in the absence of target. Indeed, the change of stripping peak current showed the maximum value at a reaction temperature of 37 °C, at which MboI has good enzymatic activity.[38] Thus 37 °C was chosen as the optimal temperature.

To further verify the result of the above electrochemical analysis, a gel electrophoresis experiment was performed. After reaction for 2 h, the product mixtures were applied to a polyacrylamide gel (PAGE). All the gel images recorded at 110 mV for 1 h showed the bands of primers 1 and 2 (Figure 4A, inset). In the presence of target DNA, the band of the cleavage product did not occur at the temperature of 45 °C, whereas the band could be observed at both 37 and

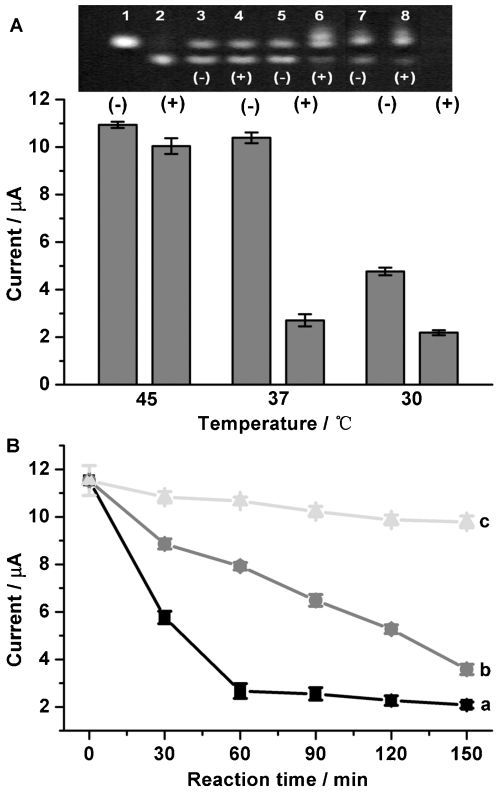

Figure 4. A) Stripping peak currents obtained at the recycling temperatures of 45, 37, and 30 °C for 1 h with (+) and without (−) the presence of 1 pM target. Inset: Non-denaturing PAGE analysis of primer 2, primer 1, and the products digested by MboI with (+) and without (−) the presence of target at 45, 37, and 30 °C for 2 h from left to right in 1× TBE buffer at 110 mV for 1 h. B) Dependence of the stripping peak current on reaction time at the target concentration of a) 1.0, b) 0.01, and c) 0 pM.

30 °C. At 30 °C, the band of the cleavage product occurred even in the absence of target DNA with excessive amounts of MboI. The results were consistent with the conclusion of the electrochemical analysis.

The reaction progress of endonuclease-assisted target recycling could be monitored by performing the competitive hybridization on the sensor surface after target recycling for different durations of time. As shown in Figure 4B, as the target recycling time increased, the stripping peak current decreased. The rate of decrease depended on the concentration of target DNA. In the presence of 1 pM target, the decrease reached a plateau at 60 min (Figure 4B, curve a). The stripping peak current showed a very slow decrease in the absence of target (Figure 4B, curve c), thus verifying the assumption that MboI does not cleave the single strands and the hybridization of primer 1 and primer 2 in the absence of target DNA is thermodynamically unstable at the selected temperature. To ensure the performance of the sensing system over a wide range of concentrations, 90 min was chosen as the optimal reaction time.

Analytical performance: The typical linear potential sweep curves obtained at different concentrations of target DNA

under the optimal conditions are shown in Figure 5A. The stripping response decreased as the concentration of target DNA increased. The plot of the peak current versus the logarithm of the target concentration showed a linear relation-

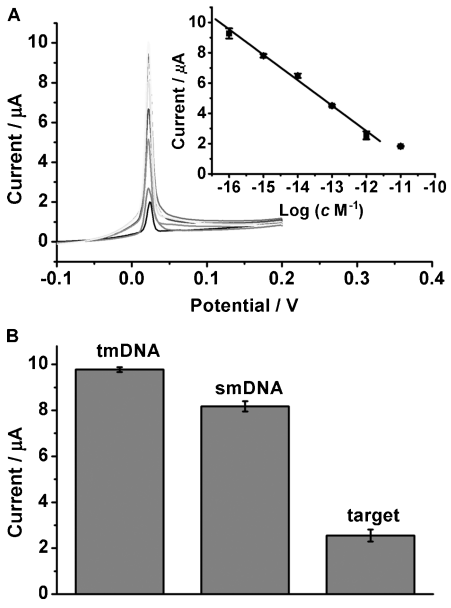

Figure 5. A) Linear potential sweep curves at target DNA concentrations of 10, 1, 0.1, 0.01 pM, and 1, 0.1, 0.01 fM from bottom to top. Inset: Linear relationship between peak currents and logarithm of target concentrations ($n=3$). B) Stripping peak current at 1 pM of the complement sequence, single-base mismatched sequence, and three-base mismatched sequence.

ship in the range from 0.1 to 1000 fM (Figure 5A, inset). The detection limit was calculated to be 0.066 fM (3σ). This low detection limit resulted from the dual signal amplification of endonuclease-assisted target recycling and highly loaded AgNPs on CNSs.

Selectivity is an important parameter for a sensing system. The specificity of the proposed DNA sensing system was investigated by performing the endonuclease-assisted target recycling with three kinds of DNA sequences, including a perfect complementary target, single-base mismatched oligonucleotide (smDNA), and three-base mismatched oligonucleotide (tmDNA) at the same concentration (1 pM). As shown in Figure 5B, the smDNA and tmDNA exhibited signals 3.2-fold and 3.8-fold greater than that of the perfect complementary target, respectively, which indicated good sensing performance in discriminating between perfect complementary target and the base mismatched oligonucleotides.

Conclusion

A simple competitive format was designed for ultrasensitive detection of sequence-specific DNA by combining homogeneous endonuclease-assisted target DNA recycling with streptavidin-functionalized AgNP-tagged CNSs as a label for electrochemical stripping analysis. The Y-junction structure formed at the optimal temperature could produce a large amount of target-sequence-independent product for signal amplification with the assistance of endonuclease. The signal tag could be synthesized by means of in situ reduction of Ag^+ adsorbed onto negatively charged polyelectrolyte-layer-assembled CNSs. Both the high loading of AgNPs on the CNS surface and the target DNA recycling amplified the detection signal. On the basis of the competition between biotin-labeled primer 1 and its cleaved product, the proposed strategy had good performance with a low detection limit, a wide linear range, and excellent selectivity for base discrimination, thereby offering potential applications in bioanalysis and biomedicine.

Experimental Section

Materials and reagents: Tris(2-carboxyethyl)phosphine hydrochloride (TCEP), poly(allylamine hydrochloride) (PAH), poly(sodium 4-styrenesulfonate) (PSS), hexaammineruthenium(III) chloride (RuHex), and 6-mercaptohexanol (MCH) were purchased from Sigma–Aldrich, Inc. (USA). FastDigest enzyme MboI and 10×FastDigest buffer were obtained from Fermentas Inc. (Canada). Streptavidin was purchased from Promega, Inc. (USA). Silver nitrate and trisodium citrate were obtained from Nanjing Chemical Reagent Co. Ltd. (Nanjing, China). Tris(hydroxymethyl)aminomethane (tris)-HCl (10 mM, pH 7.4) that contained 1 mM ethylenediaminetetraacetic acid (EDTA) and 50 mM NaCl was used as the DNA immobilization buffer. Tween-20 (0.05 % v/v) was spiked into phosphate-buffered saline (10 mM PB, 50 mM NaCl) as wash buffer (PBST) to minimize nonspecific adsorption. In our experiments, 1 mM MCH in 10 mM Tris-HCl (pH 7.4) was used to assemble MCH on a gold electrode. Throughout the experiments, 1.0 M KCl solution was used as the detection electrolyte, whereas 50 μM RuHex in 10 mM Tris-HCl (pH 7.0) was used for determination of the surface density of the capture probe modified on gold electrodes. All other reagents were of analytical grade. All aqueous solutions were prepared using ultrapure water (18 MΩ, Milli-Q, Millipore). The oligonucleotides were purchased from Sangon Biological Engineering Technology Co. Ltd. (Shanghai, China) and purified using high-performance liquid chromatography. Their sequences were as follows: three-base mismatched oligonucleotide: 5′CCG ATG AGA CGT TTC CCT TCG AC3′; single-base mismatched oligonucleotide: 5′CCG AAG AGA CCT TTC CCT TCG AC3′; target: 5′CCG AAG AGA CCT TTC CGT TCG AC3′; capture probe: 5′HS-C_6CACCACAACCCGCCCGAT3′; primer 1: 5′biotin-GTCGAACG-GATTTGATCGGGCGGGTTGTGGTG3′; and primer 2: 5′AAAA-GATCAAAAAGGTCTCTTCGG.

Apparatus: The morphologies of CNSs and AgNP-tagged CNSs were examined using a Hitachi S-4800 SEM (Japan). The morphology of AgNP-tagged CNSs was recorded using a JEM 2100 TEM. Fourier transform infrared spectra were recorded using a Nicolet 400 Fourier transform infrared spectrometer (Madison, WI). XPS measurements were performed using a PHI5000 Versa Probe spectrometer (ULVAC-PHI, Japan). Electrochemical measurements were carried out at room temperature using a CHI 630A electrochemical workstation (Chenhua, Shanghai, China) with a conventional three-electrode cell. The three-electrode electrochemical cell consisted of a gold working electrode (2 mm in diameter), a platinum counter electrode, and a saturated calomel reference electrode (SCE).

Synthesis of CNSs: The monodispersed CNSs were prepared by hydrothermal synthesis according to a previous report.[32] Briefly, glucose solution (30 mL, 0.5 M) was added into a 40 mL autoclave, which was then kept in an oven of 180 °C for 4 h. After being cooled in air, the product

was purified by repeated centrifugation/redispersion cycles with ultrapure water and anhydrous ethanol, and finally dried at 40 °C in an oven.

Preparation of streptavidin-functionalized AgNP-tagged CNSs: The dispersion of CNSs (1 mL, 1 mg mL^{-1}) was mixed with PAH solution (1 mL, 1 mg mL^{-1} in 0.5 M NaCl) and incubated for 30 min. After centrifugation three times with ultrapure water to remove the excess amount of polyelectrolyte, the resulting CNSs were mixed with PSS solution (1 mL, 1 mg mL^{-1} in 0.5 M NaCl) and was then incubated for another 30 min. After separation from the excess amount of PSS, $AgNO_3$ solution (80 μL, 0.1 M) was added into the resulting dispersion in water (1 mL), and the mixture was stirred for 30 min. Finally, 1% (v/v) trisodium citrate solution (10 mL) was added to the mixture under stirring. It was then heated to 100 °C and kept at this temperature for 60 min. The precipitate was collected by centrifugation, washed twice with ultrapure water, and redispersed in water (5 mL). Afterwards, streptavidin (50 μL, 0.5 mg mL^{-1}) was added to the dispersion and incubated for 2 h at room temperature under stirring. After centrifugation and washing with water three times, the obtained streptavidin-functionalized AgNP-tagged CNS was dispersed in PB solution (pH 7.4) and stored at 4 °C.

Electrode fabrication: The gold electrode was polished thoroughly with 0.05 μm alumina powder, followed by ultrasonic cleaning with anhydrous ethanol and Milli-Q water for 2 min each to remove the residual alumina powder. The electrode was then electrochemically pretreated by performing a cyclic scan between 0 and +1.6 V at 100 mV s^{-1} in 1 M H_2SO_4. After rinsing thoroughly and drying with a pure nitrogen, the thiolated capture probe, which was activated with 1 M TCEP for 1 h, was pipetted onto the electrode surface and incubated in 100% humidity for 3 h. The capture-probe-modified electrode was blocked by immersing it in a 1 M MCH solution for 1 h and then washing it with PBST to completely remove any nonspecifically adsorbed materials.

Endonuclease-assisted target recycling and electrochemical measurements: The endonuclease-assisted target DNA recycling was performed in a solution (20 μL) that consisted of primer 1 (1.0 nM), primer 2 (1.0 nM), the target at different concentrations, FastDigest enzyme MboI (1 μL), and 10×FastDigest buffer (2 μL). After being mixed gently and spun down, the mixture was incubated at 37 °C for a certain time and heated at 65 °C for 15 min to end the recycling. Next, the resulting solution (5 μL) was applied to the capture-probe-modified gold electrodes and incubated at room temperature for 2 h. After rinsing the electrode thoroughly with PBST, streptavidin-functionalized AgNP-tagged CNSs (5 μL, 0.2 mg mL^{-1}) were applied to the surface and incubated for 30 min, which was then washed with PBST to perform the stripping analysis by potential sweep from −0.15 to 0.20 V at 50 mV s^{-1} in 1.0 M KCl solution.

Acknowledgements

This work was funded by the National Basic Research Program of China (2010CB732400), the National Natural Science Foundation of China (21121091, 21135002), and the Natural Science Foundation of Jiangsu (BK2010302).

[1] J. Wu, S. Campuzano, C. Halford, D. A. Haake, J. Wang, *Anal. Chem.* **2010**, *82*, 8830–8837.
[2] L. H. Xiao, L. Wei, Y. He, E. S. Yeung, *Anal. Chem.* **2010**, *82*, 6308–6314.
[3] B. J. Zou, Y. J. Ma, H. P. Wu, G. H. Zhou, *Angew. Chem.* **2011**, *123*, 7533–7536; *Angew. Chem. Int. Ed.* **2011**, *50*, 7395–7398.
[4] J. Huang, Y. R. Wu, Y. Chen, Z. Zhu, X. H. Yang, C. Y. J. Yang, K. M. Wang, W. H. Tan, *Angew. Chem.* **2011**, *123*, 421–424; *Angew. Chem. Int. Ed.* **2011**, *50*, 401–404.
[5] P. Harding Lepage, R. Peytavi, M. G. Bergeron, M. Leclerc, *Anal. Chem.* **2011**, *83*, 8086–8092.
[6] A. E. Prigodich, A. H. Alhasan, C. A. Mirkin, *J. Am. Chem. Soc.* **2011**, *133*, 2120–2123.
[7] F. A. Wang, J. Elbaz, R. Orbach, N. Magen, I. Willner, *J. Am. Chem. Soc.* **2011**, *133*, 17149–17151.
[8] S. W. Bae, M. S. Cho, S. S. Hur, C. B. Chae, D. S. Chung, W. S. Yeo, J. I. Hong, *Chem. Eur. J.* **2010**, *16*, 11572–11575.
[9] H. Li, Z. Y. Sun, W. Y. Zhong, N. Hao, D. K. Xu, H. Y. Chen, *Anal. Chem.* **2010**, *82*, 5477–5483.
[10] F. Divsar, H. X. Ju, *Chem. Commun.* **2011**, *47*, 9879–9881.
[11] J. H. Chen, J. Zhang, Y. Guo, J. Li, F. F. Fu, H. H. Yang, G. N. Chen, *Chem. Commun.* **2011**, *47*, 8004–8006.
[12] R. Z. Fu, T. H. Li, S. S. Lee, H. G. Park, *Anal. Chem.* **2011**, *83*, 494–500.
[13] C. Q. Zhao, L. Wu, J. S. Ren, X. G. Qu, *Chem. Commun.* **2011**, *47*, 5461–5463.
[14] T. Kiesling, K. Cox, E. A. Davidson, K. Dretchen, G. Grater, S. Hibbard, R. S. Lasken, J. Leshin, E. Skowronski, M. Danielsen, *Nucleic Acids Res.* **2007**, *35*, e117.
[15] W. Xu, X. J. Xue, T. H. Li, H. Q. Zeng, X. G. Liu, *Angew. Chem.* **2009**, *121*, 6981–6984; *Angew. Chem. Int. Ed.* **2009**, *48*, 6849–6852.
[16] J. H. Chen, J. Zhang, J. Li, F. F. Fu, H. H. Yang, G. N. Chen, *Chem. Commun.* **2010**, *46*, 5939–5941.
[17] R. M. Kong, X. B. Zhang, Z. Chen, H. M. Meng, Z. L. Song, W. H. Tan, G. L. Shen, R. Q. Yu, *Anal. Chem.* **2011**, *83*, 7603–7607.
[18] Z. Y. Liu, W. Zhang, S. Y. Zhu, L. Zhang, L. Z. Hu, S. Parveen, G. B. Xu, *Biosens. Bioelectron.* **2011**, *29*, 215–218.
[19] Q. P. Guo, X. H. Yang, K. M. Wang, W. H. Tan, W. Li, H. X. Tang, H. M. Li, *Nucleic Acids Res.* **2009**, *37*, e20.
[20] A. R. Connolly, M. Trau, *Angew. Chem.* **2010**, *122*, 2780–2783; *Angew. Chem. Int. Ed.* **2010**, *49*, 2720–2723.
[21] R. Ren, C. C. Leng, S. S. Zhang, *Chem. Commun.* **2010**, *46*, 5758–5760.
[22] X. L. Zuo, F. Xia, Y. Xiao, K. W. Plaxco, *J. Am. Chem. Soc.* **2010**, *132*, 1816–1818.
[23] J. Su, H. J. Zhang, B. Y. Jiang, H. Z. Zheng, Y. Q. Chai, R. Yuan, Y. Xiang, *Biosens. Bioelectron.* **2011**, *29*, 184–188.
[24] C. Y. J. Yang, L. Cui, J. H. Huang, L. Yan, X. Y. Lin, C. M. Wang, W. Y. Zhang, H. Z. Kang, *Biosens. Bioelectron.* **2011**, *27*, 119–124.
[25] Y. F. Wu, C. L. Chen, S. Q. Liu, *Anal. Chem.* **2009**, *81*, 1600–1607.
[26] H. F. Dong, F. Yan, H. X. Ji, D. K. Y. Wong, H. X. Ju, *Adv. Funct. Mater.* **2010**, *20*, 1173–1179.
[27] G. S. Lai, J. Wu, H. X. Ju, F. Yan, *Adv. Funct. Mater.* **2011**, *21*, 2938–2943.
[28] C. Zong, J. Wu, C. Wang, H. X. Ju, F. Yan, *Anal. Chem.* **2012**, *84*, 2410–2415.
[29] R. J. Cui, C. Liu, J. M. Shen, D. Gao, J. J. Zhu, H. Y. Chen, *Adv. Funct. Mater.* **2008**, *18*, 2197–2204.
[30] D. Du, Z. X. Zou, Y. S. Shin, J. Wang, H. Wu, M. H. Engelhard, J. Liu, I. A. Aksay, Y. H. Lin, *Anal. Chem.* **2010**, *82*, 2989–2995.
[31] Q. N. Xu, F. Yan, J. P. Lei, C. Leng, H. X. Ju, *Chem. Eur. J.* **2012**, *18*, 4994–4998.
[32] X. M. Sun, Y. D. Li, *Angew. Chem.* **2004**, *116*, 607–611; *Angew. Chem. Int. Ed.* **2004**, *43*, 597–601.
[33] S. Nakayama, L. Yan, H. O. Sintim, *J. Am. Chem. Soc.* **2008**, *130*, 12560–12561.
[34] Q. Wang, L. J. Yang, X. H. Yang, K. M. Wang, L. L. He, J. Q. Zhu, T. Y. Su, *Chem. Commun.* **2012**, *48*, 2982–2984.
[35] U. Rant, K. Arinaga, S. Fujita, N. Yokoyama, G. Abstreiter, M. Tornow, *Langmuir* **2004**, *20*, 10086–10092.
[36] R. J. Lao, S. P. Song, H. P. Wu, L. H. Wang, Z. Z. Zhang, L. He, C. H. Fan, *Anal. Chem.* **2005**, *77*, 6475–6480.
[37] A. B. Steel, T. M. Herne, M. J. Tarlov, *Anal. Chem.* **1998**, *70*, 4670–4677.
[38] K. Kato, *Nucleic Acids Res.* **1997**, *25*, 4694–4696.

Received: April 17, 2012
Published online: September 17, 2012

